PROTEINS: Structure, Function, and Genetics 30:61–73 (1998)

# Exploring Hydrophobic Sites in Proteins With Xenon or Krypton

**Thierry Prangé,[1]* Marc Schiltz,[1] Lucile Pernot,[1] Nathalie Colloc'h,[2] Sonia Longhi,[3] William Bourguet,[4] and Roger Fourme[1]**
[1]*LURE, Université Paris-Sud, 91405-Orsay Cedex, France*
[2]*LMCP, 75252-Paris Cedex 5, France*
[3]*AFMB-CNRS, UPR 9039, 13402 Marseille Cedex, France*
[4]*IGBMC, UPR de Biologie Structurale, 67404-Illkirch Cedex, France*

***ABSTRACT*** **X-ray diffraction is used to study the binding of xenon and krypton to a variety of crystallised proteins: porcine pancreatic elastase; subtilisin Carlsberg from *Bacillus licheniformis;* cutinase from *Fusarium solani;* collagenase from *Hypoderma lineatum;* hen egg lysozyme, the lipoamide dehydrogenase domain from the outer membrane protein P64k from *Neisseria meningitidis;* urate-oxidase from *Aspergillus flavus,* mosquitocidal δ-endotoxin CytB from *Bacillus thuringiensis* and the ligand-binding domain of the human nuclear retinoid-X receptor RXR-α. Under gas pressures ranging from 8 to 20 bar, xenon is able to bind to discrete sites in hydrophobic cavities, ligand and substrate binding pockets, and into the pore of channel-like structures. These xenon complexes can be used to map hydrophobic sites in proteins, or as heavy-atom derivatives in the isomorphous replacement method of structure determination. Proteins 30:61–73, 1998.**


**Key words: xenon; krypton; hydrophobic cavity; protein-ligand binding**

## INTRODUCTION

A large number of proteins are known to fix small exotic ligands, like organic solvent molecules, and several crystal structures of these complexes have been refined and deposited with the Protein Data Bank.[2] The pioneering crystallographic studies of Schoenborn and co-workers demonstrated that sperm whale myoglobin and horse haemoglobin crystals can bind xenon under moderate pressure, through weak van der Waals forces.[55,58,60,75] These xenon complexes were obtained by subjecting native protein crystals to a relatively low gas pressure (2–2.5 bar).§ Xenon was shown to bind to pre-existing atomic-sized cavities in the interior of these globular protein molecules. The interaction of xenon with proteins is the result of non-covalent, weak-energy van der Waals forces,[12,66,67] and therefore, the process of xenon binding is completely reversible.[39,64] The xenon complex with myoglobin has been studied in detail by Tilton and co-workers,[64,66–68] who showed that the number and the occupancies of xenon binding sites vary with the applied pressure. Thus, at a pressure of 7 bar, one major (almost fully occupied) and three secondary (half-occupied) sites were found. Xenon binds to myoglobin with very little perturbation of the surrounding molecular structure. Hence, the xenon complex is highly isomorphous with the native protein structure. Cyclopropane and dichloromethane have also been shown to bind to the major xenon binding site in myoglobin,[42,56,57] but the greater size of these molecules causes some distortions in the surrounding protein structure and rearrangement of some amino acid side chains. Even a single nitrogen molecule binds to this same site at a pressure of 145 bar.[65] Xenon was also described to bind to serum albumin,[9] renin, and tobacco mosaic virus,[57,59] but no structural studies have been undertaken on these complexes.

Due to its anesthetic properties,[11] xenon has been used extensively as a prototype for theoretical and experimental studies on the interactions of anesthetics with proteins.[13,14] The structural investigations of xenon, cyclopropane, and dichloromethane binding to myoglobin and hemoglobin, along with the crystallographic analysis of halothane binding into the enzymatic site of adenylate kinase,[47] provide, so far, good examples of the interaction of general anesthetics to specific sites in proteins. The nature of the molecular site of general anesthesia is still a matter of important debate,[18,38] but over the last decade, evidence has been accumulated in support of the theory that general anesthetics act by binding directly to proteins,[17,18] rather than by perturbing lipid bilayers in synaptic membranes, as it was

§Non SI-units used in this article: 1 bar = $10^5$ Pa, 1 Å = $10^{-10}$ m.

Contract grant sponsor: CNRS/MR/CEA (Action Concertee des Sciences du Vivant 5); Contract grant sponsor: NATO.
*Correspondence to: Thierry Prange, LURE, Bât. 209d, Université Paris-Sud, 91405-Orsay Cedex, France. E-mail: prange@lure.u-psud.fr
Received 22 October 1996; Accepted 29 April 1997

thought before.[76] More recently, the considerable development in medicine of Magnetic Resonance Imaging (MRI) techniques led to a re-investigation of xenon as a probe in imaging and diagnostic techniques.[30,77]

Protein-xenon complexes can be used as highly isomorphous heavy-atom derivatives for solving the phase problem in X-ray crystallography.[48,50,52,53,63,70] Xenon has now been used successfully as a heavy-atom in the structure determination of the human nuclear retinoid-X receptor RXR-α ligand binding domain,[3] the molybdoenzyme DMSO reductase from *Rhodobacter spheroides*,[54] the oligomerization domain of the cartilage oligomeric matrix protein (COMP),[34] the Photosystem I from *Synechoccus elongatus*,[25] the lipoamide dehydrogenase domain from the outer membrane protein P64k of the bacteria *Neisseria meningitidis*,[33] and the enzyme urate-oxidase from *Aspergillus flavus*.[8]

Until recently, structural studies on protein-xenon complexes had been limited exclusively to the cases of myoglobin and hemoglobin. Binding of xenon into the enzymatic site of serine proteinases has been reported by Schiltz et al.[51] The present study describes and compares the xenon and krypton binding sites in a variety of proteins: porcine pancreatic elastase, subtilisin Carlsberg from *Bacillus licheniformis*, cutinase from *Fusarium solani* (wild type and S120A mutant), collagenase from *Hypoderma lineatum*, hen egg-white lysozyme, the lipoamide dehydrogenase domain of the outer membrane protein P64k from *Neisseria meningitidis*, urate oxidase from *Aspergillus flavus*, mosquitocidal δ-endotoxin CytB from *Bacillus thuringiensis* sp. *kyushuensis* and the ligand-binding domain of the human nuclear retinoid-X receptor RXR-α.† These are proteins whose native three-dimensional structures have been determined by x-ray crystallography and refined to resolutions equal or better than 2.7Å. [3,4,8,26,31,33,35,37,78]

## MATERIALS AND METHODS

### Sample Preparation and X-Ray Data Collection

Standard procedures, described in the literature were used to grow crystals of elastase,[37] Subtilisin,[44] lysozyme,[62] and P64k.[32] Crystals of cutinase,[35] collagenase,[4] RXR,[3] urate oxidase,[8] and CytB[31] were obtained from the crystallographic groups who solved the structures. For cutinase, the xenon binding was investigated on the wild type protein as well as on the mutant S120A, where the active site serine is replaced by alanine. Crystals of this mutant are isomorphous to the native ones.[36]

The method used to prepare xenon derivatives has been described earlier.[50] Native crystals, mounted in quartz capillaries, fitted to a specially designed cell, were submitted to gas pressure a few minutes before starting the data collection.‡ The gas pressure was maintained during the data collection. Native and derivative data were collected under similar conditions.

Krypton complexes were prepared for elastase and lysozyme at pressures of 48–56 bars.[52]

Diffraction data were collected at the DW32 wiggler beam-line at the LURE synchrotron facility in Orsay, France[16] using x-rays at a wavelength of 0.9 A and a MAR-Research image plate detector. Diffraction data were processed with the MOSFLM program.[29] Data reduction and merging as well as all subsequent crystallographic computations were carried out with programs of the CCP4 package.[6] A summary of the X-ray data collections on all samples is given in Table I.

### Xenon and Krypton Site Determination

The coordinates of the major xenon sites were located by difference-Fourier calculations using the $|F_{deriv}| - |F_{native}|$ terms as amplitudes and $\phi_{native}$ as phases (known native structures were from the Protein Data Bank[2]: codes for elastase, lysozyme, subtilisin, cutinase, collagenase, CytB and RXR were 6EST, 1LSE, 1SCA, 1CUS, 1HYL, 1CBY and 1LBD respectively).

### Refinements of the Xenon/Krypton Sites

Structure refinements of elastase/Xe, subtilisin/Xe, collagenase/Xe, urate oxidase/Xe, and lysozyme/Xe complexes were carried out by the method of simulated annealing with the XPLOR program.[5] The native structures inclusive of the previously located xenon/krypton atoms and exclusive of water molecules were used as starting models. At regular intervals, water molecules were identified by difference Fourier-calculations and added to the model. As occupancies and thermal factors are highly correlated, the xenon atoms were assigned a fixed thermal factor equal to the average thermal factor $<B_W>$ of the crystallographically refined water molecules. The xenon occupancy factor was adjusted periodically, so that its B remains within a few Å$^2$ equal to the recalculated $<B_W>$. So, there is a constant adjustment of the occupancy factor. The final stages of the refinements were carried out using the stereochemically restrained least-squares minimization method with the PROLSQ program.[19] The data given in Table I represent only a brief summary of these refinements. The full details are reported in

†For simplicity and clarity, the following short names will be used hereafter: elastase, subtilisin, cutinase, collagenase, lysozyme, P64k, urate-oxidase, CytB, and RXR. COMP is an abbreviation for cartilage oligomeric matrix protein.

‡A detailed description of the pressure cell and accessories can be found at the Internet site http://www.lure.u-psud.fr/WWW_ROOT/DOCUMENTS/lure/sections/xenon/xenon.html

**TABLE I. Xenon-Protein Complexes: Summary of Structural Data***

| Protein | No. of residues | Xe gas pressure (bar) | No. of sites | Refinement of Xe complexes: Final R-factor (%) | Refinement of Xe complexes: High-resolution limit (Å) | Refinement of Xe complexes: No. of reflections used |
|---|---|---|---|---|---|---|
| Elastase | 240 | 8 | 1 | 18.3 | 2.2 | 10,937 |
| Subtilisin | 275 | 12 | 1 | 19.4 | 2.08 | 9,665 |
| Collagenase | 2 × 230 | 12 | 2 × 1 | 19.7 | 2.53 | 17,432 |
| Cutinase (wild-type) | 196 | 12 | 1 | n.r. | — | — |
| Cutinase (S120A) | 196 | 12 | 1 | n.r. | — | — |
| Urate-oxidase | 4 × 301 | 8 | 4 × 1 | 21.0 | 2.3 | 18,523 |
| P64k | 2 × 481 | 13 | 2 × 2 | n.r. | — | — |
| Lysozyme | 129 | 12 | 4 | 16.8 | 2.1 | 6,521 |
| RXR | 2 × 238 | 20 | 2 × 2 | n.r. | — | — |
| CytB | 2 × 259 | 10 | 1 | n.r. | — | — |

*The refined structures have been deposited with the Protein Data Bank (n.r. = not refined).

the header of each deposited file within the Protein Data Bank, Brookhaven.

For P64k, the xenon complex was used as a heavy-atom derivative for the resolution of the crystal structure,[33] and during the phasing process, the xenon sites were refined with the program MLPHARE.[43] Strictly speaking, however, the diffraction data were not on an absolute scale, so that the reported occupancies of the xenon atoms may not serve for comparisons with sites in other proteins. For cutinase, the xenon atoms were also refined with MLPHARE, but in this case, high-resolution data had been collected (up to 1.6Å), so that the structure factor amplitudes could be put on an absolute scale by a Wilson plot.

Xenon complexes of DMSO reductase[54] and COMP[34] were described in the literature.

Dr. Schindelin (California Institute of Technology, Passadena, CA, USA) has kindly communicated the co-ordinates of the Xe atom in DMSO reductase to us to include the description of this site in Table II.

## RESULTS

Table II summarizes the short contacts observed within a range of c.a. 4.5 Å around the xenon atom at each site. If we add the case of the DMSO-reductase,[54] we remark that hydrophobic contacts are dominant (57 over a total of 77). When the size of the cavities is rather small (i.e., in RXR), it can accommodate only one single atom in a well-ordered position. The observed electron density in the difference-Fourier maps, corresponding to the xenon atom, usually has the shape of a sphere or ellipsoid. However, when the cavity is much larger than the volume of a single xenon or krypton atom, disordered positions are observed as in mutants of phage T4 lysozyme.[45]

The various binding cavities corresponding to the data gathered in Table II are depicted in Figures 1 to 7. The most frequent side chains in interaction are from Ala (6), Leu (21), Val (11), Ile (9), or Phe (5) residues, or Ser, in the special case of serine proteinases.

## DISCUSSION

One of the most puzzling features of xenon binding to proteins is the large diversity of the binding sites. Xenon binds to intra- as well as to inter-molecular sites, to closed inaccessible cavities, as well as to exposed pockets and even into channel-pores. The binding sites may be lined up exclusively by aliphatic residues, or they also may include aromatic, or, polar groups. Xenon may bind into void sites, or replace existing water molecules. Below, we have attempted to classify the various binding sites into subsets according to their common features.

### Definition

A *cavity* is a region in a protein that is not occupied by protein atoms and that is entirely closed off by the protein. By definition, a cavity is *inaccessible* from the outside, in the static description of a crystal structure. In contrast, a *pocket* (sometimes called *surface invagination*) is connected (*accessible*) to the outside. A pocket would only become a closed cavity if the atomic radii of the protein atoms that delimit the cavity were to be increased. In order to test whether binding sites are cavities or pockets, molecular surfaces were calculated with the Connolly algorithm.[10] Cavities are delimited by closed surface patches that have no connection to the outer molecular surface.

It is well known that the atoms in the interior of protein molecules are densely packed, and that these regions are more similar to solids than to organic liquids. Calculations presented by Klapper[22] have estimated that there is twice as much free volume distributed throughout simple organic liquids than in proteins. However, in proteins, the free volume does not need to be distributed randomly (as in liquids), and empty intramolecular cavities exist in numerous proteins.[21,23] These cavities exist at the

**TABLE II. Closest Contacts (Å) Around the Xenon (or Krypton) Atoms in the Various Binding Sites, Within a Sphere of 4.5–4.7 Å**

| Protein | Atom | Atom (resid.) | Dist. | Atom (resid.) | Dist. | B/Occ* |
|---|---|---|---|---|---|---|
| Elastase | Xe | Oγ(S195) | 3.40 | O(C191) | 3.71 | 22.6/0.81 |
| | | Cγ2(V216) | 3.89 | Cγ2(T213) | 4.0 | |
| Elastase | Kr | Oγ(S195) | 3.28 | O(C191) | 3.90 | 18.9/0.49† |
| | | Cγ2(V216) | 3.75 | Cγ2(T213) | 3.85 | |
| Subtilisin | Xe | Oγ(S221) | 4.03 | Cβ(A152) | 3.94 | 29.3/0.71 |
| | | Cα(G154) | 3.92 | Nδ2(N155) | 3.73 | |
| | | Oγ2(T220) | 4.11 | Cα(L126) | 3.99 | |
| | | Ow(310) | 4.43 | | | |
| Cutinase (native) | Xe | Oγ(S120) | 4.24 | Nδ2(N84) | 3.33 | 19.1/0.81‡ |
| | | Cγ2(T150) | 4.19 | Cγ1(V177) | 4.17 | |
| | | Cδ2(L182) | 3.99 | | | |
| Collagenase | Xe | Subunit-A: | | Subunit B: | | |
| | | Oγ(S195a) | 3.67 | Oγ(S195b) | 3.51 | 28.1/0.95 (in site A) |
| | | Cγ2(V216a) | 3.98 | Cγ2(V216b) | 4.01 | |
| | | Cγ1(V213a) | 4.22 | Cγ1(V213b) | 4.33 | |
| | | Oϵ1(Q37b) | 3.76 | Oϵ1(Q37a) | 4.0 | 31.8/0.80 (in site B) |
| | | O(S214a) | 4.53 | O(S214b) | 4.58 | |
| | | C(C191a) | 4.29 | C(C191b) | 4.27 | |
| | | Ow(234) | 3.87 | Ow(552) | 4.40 | |
| Urate-oxidase | Xe | Cδ2(L178) | 4.33 | Cγ2(T180) | 4.79 | 30.5/0.85 |
| | | Cδ1(F219) | 4.12 | Cγ1(V227) | 4.14 | |
| | | Cγ2(T230) | 3.99 | Cδ2(L252) | 3.68 | |
| P64k | Xe | | | | | |
| Site #1 | | Cδ2(L323) | 3.42 | Cβ(A176) | 3.88 | 22.5/0.55‡ |
| | | Cβ(V319) | 4.59 | O(L172) | 3.66 | |
| | | Cd1(I179) | 4.60 | Cδ2(L202) | 3.81 | |
| | | Cβ(N175) | 4.00 | Cγ(L172) | 4.57 | |
| Site #2 | | Cδ(L327) | 3.60 | Cζ(F356) | 2.65 | 30.5/0.40‡ |
| | | C(W348) | 3.70 | Cϵ(R355) | 3.66 | |
| | | Oγ1(T318) | 3.25 | N(L314) | 3.45 | |
| Lysozyme | Kr | Cγ2(V92) | 3.12 | Cδ1(L56) | 3.38 | 19/0.49 |
| | | Cγ2(I55) | 3.46 | Cδ1(I88) | 4.16 | |
| | | Cϵ(M12) | 3.55 | Cβ(S91) | 3.89 | |
| Lysozyme | Xe | | | | | |
| Site #1 | | Oγ1(T43) | 3.65 | Cβ(T43) | 4.00 | 36.2/0.33 |
| (intermolecular) | | N(R45) | 4.25 | N(N44) | 4.36 | |
| | | Cγ2(T51) | 4.55 | Nh2(R68) | 4.49 | |
| | | Ow(20) | 4.50 | | | |
| | | + symmetry-related | | | | |
| Site #2 | | Cγ2(V92) | 3.18 | Cδ1(L56) | 3.33 | 32.9/0.28 |
| (intramolecular) | | Cγ2(I55) | 3.51 | Cδ1(I88) | 4.19 | |
| | | Cϵ(M12) | 3.54 | Cβ(S91) | 3.91 | |
| Site #3 | | Cα(I58) | 4.30 | Nϵ1(W108) | 3.75 | 36.0/0.1 |
| (intramolecular) | | O(Q57) | 4.03 | Cδ1(W1080) | 3.96 | |
| | | Cδ1(I98) | 4.30 | O(A107) | 3.78 | |
| CytB | Xe | Cδ1(L33) | 3.4 | Cδ1(I54) | 4.2 | n.r.¶ |
| (intermolecular) | | Cδ1(I233) | 4.7 | Cζ(F237) | 3.9 | |
| | | + symmetry-related | | | | |
| RXR | Xe | | | | | |
| Site #1 | | Cγ1(V332) | 4.09 | O(S336) | 4.33 | n.r. |
| | | Cα(A337) | 3.25 | Cβ(A340) | 3.36 | |
| | | Cγ2(V342) | 3.41 | O(K440) | 3.69 | |
| | | Cδ2(L441) | 4.23 | Cβ(D444) | 3.94 | |
| Site #2 | | Cδ1(L370) | 2.92 | Cβ(R421) | 4.30 | n.r. |
| | | Cδ1(L425) | 3.78 | Cδ1(L422) | 4.62 | |
| DMSO-reductase | Xe | Cζ(F110) | 3.23 | Cβ(A428) | 3.58 | n.r. |
| | | Cγ1(V402) | 3.56 | Cϵ(M405) | 4.05 | |
| | | Cδ2(L406) | 4.21 | Cδ2(L452) | 4.23 | |
| | | Ch2(W449) | 4.29 | | | |

*Occ = occupancy factor, B = temperature factor (refined, Å$^2$) for Xe or Kr. Refined using PROLSQ.[19] Standard deviations are within 2 Å$^2$ for B factor and ±0.1 for Occ.

†Refined with program SHARP.[27]

‡Refined using program MLPHARE[43] after absolute scaling of the data.

¶n.r. = not refined.

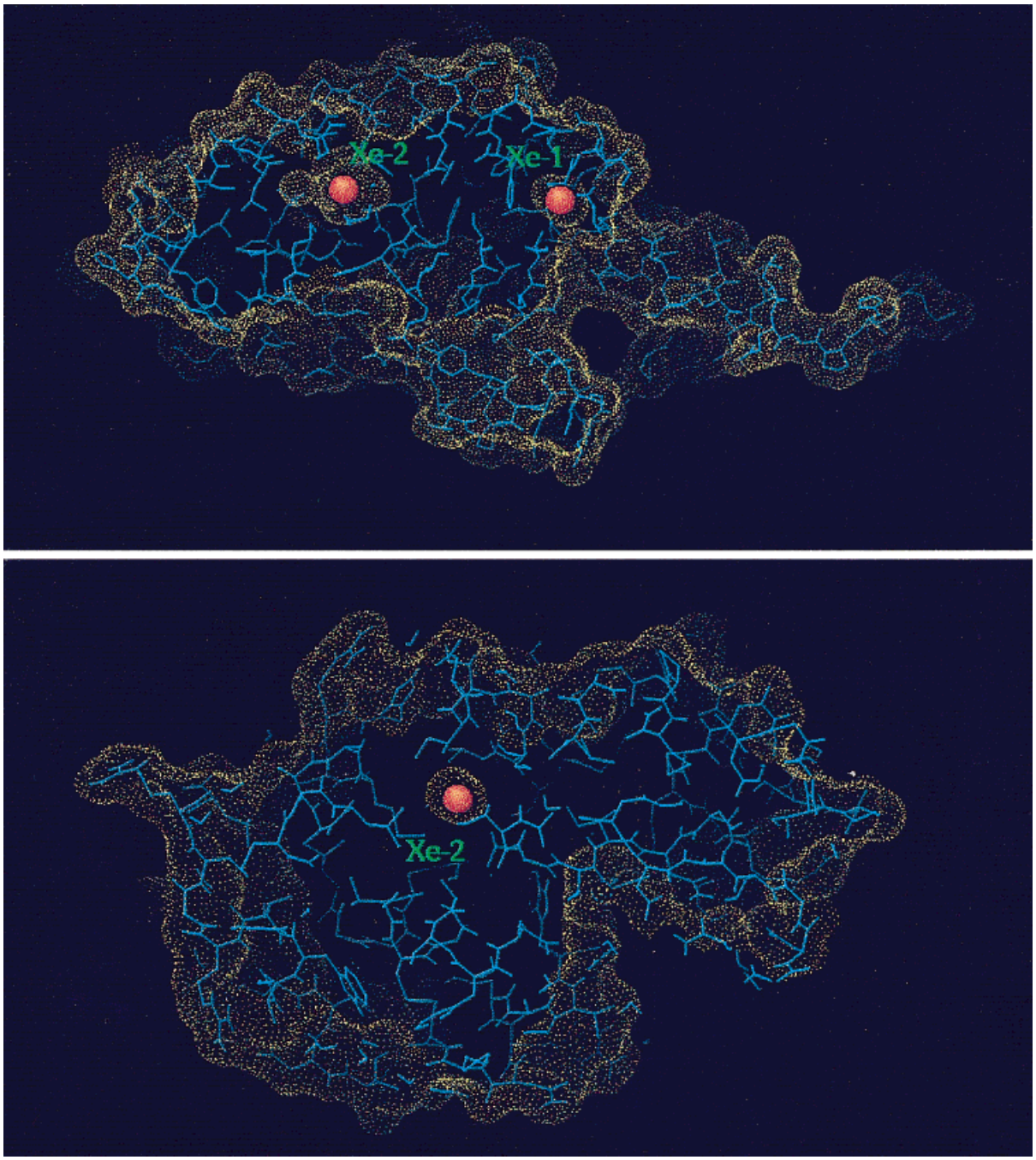


Fig. 1. View of the binding sites of xenon atoms in hen egg lysozyme (**lower**) and RXR (**upper**). The accessible surfaces are calculated by the method of Connolly.[10]

expense of considerable cost in free energy, so that it is unlikely that they are mere packing defects. The hypothesis that cavities are important for the conformational flexibility of protein molecules is supported by the characteristics of xenon binding to myoglobin. Tilton et al.[66] have observed an overall reduction in temperature factors upon xenon binding. This effect was interpreted as a ligand-induced restriction of the number of conformational states. Such an interpretation would also explain why the rotational degrees of freedom of bound water molecules in the protein decrease upon xenon binding.[79] Binding of xenon to myoglobin cavities also affects the functionality of the protein in a rather drastic way.[61]

All these observations are evidences of the importance of intramolecular cavities for the dynamics

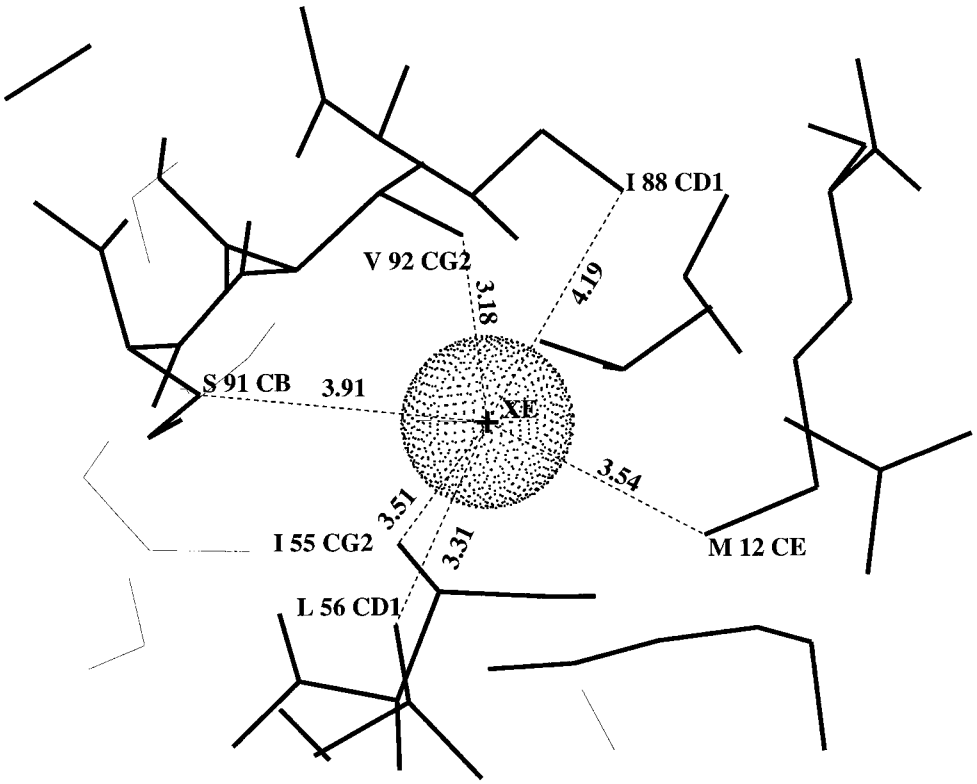


Fig. 2. The distances around the xenon in site #2 of lysozyme (the inner cavity in Fig. 1). The xenon atom is represented at its van der Waals radius.

and functionality of protein molecules. The preparation of xenon complexes provides a unique experimental method to detect and study such cavities.

### Xenon Binding Into Hydrophobic Intramolecular Cavities

The main intramolecular binding site in lysozyme (site #2 in Table II), the binding sites in urate-oxidase and P64k, one of the binding sites in RXR (site #2 in Table II), and the binding site in DMSO-reductase belong to this category. These sites are truly closed cavities (Fig. 1), similar to the binding sites observed in myoglobin and hemoglobin. The observed cavities are usually small, accomodating space for no more than one xenon atom and they do not contain ordered water molecules. Thermodynamic considerations suggest that they are also void of disordered water.[72,74] They are buried in the protein interior, sometimes at a distance of several angströms from the molecular surface, and they are thus built predominantly by hydrophobic side chains. Access to these sites is only possible via transient channels produced by concerted domain movements, as it was suggested earlier in the case of myoglobin,[64,66–68] as well as for the binding of small, organic molecules,[40,45] or molecules like benzene or indole to the interior of Phage T4 lysozyme mutants.[15] The first of these studies demonstrates that there is a correlation between the geometry of the binding cavity, and the degree of occupancy and the disorder of the ligand. The second report illustrates the influence of the protein core fluctuations on the millisecond to microsecond time scale, which allow the molecules to easily reach the core region of the protein.

The binding equilibrium of xenon to proteins has been analyzed both theoretically[20,67] and experimentally.[50,51,52,64,66]

### Xenon vs. Krypton

In elastase, krypton binds to the same site as xenon, but in order to achieve noticeable substitution, substantially higher pressures have to be applied.[52] This is probably due to the fact that krypton atoms have a smaller electronic polarizability than xenon atoms. Thus, the van der Waals forces that exist between the rare gas atoms and the protein molecules are smaller with krypton gas. In lysozyme, krypton only binds into the major intramolecular site (site #2).[52] Even at high pressures (48 bar), the three other xenon binding sites are not observed to

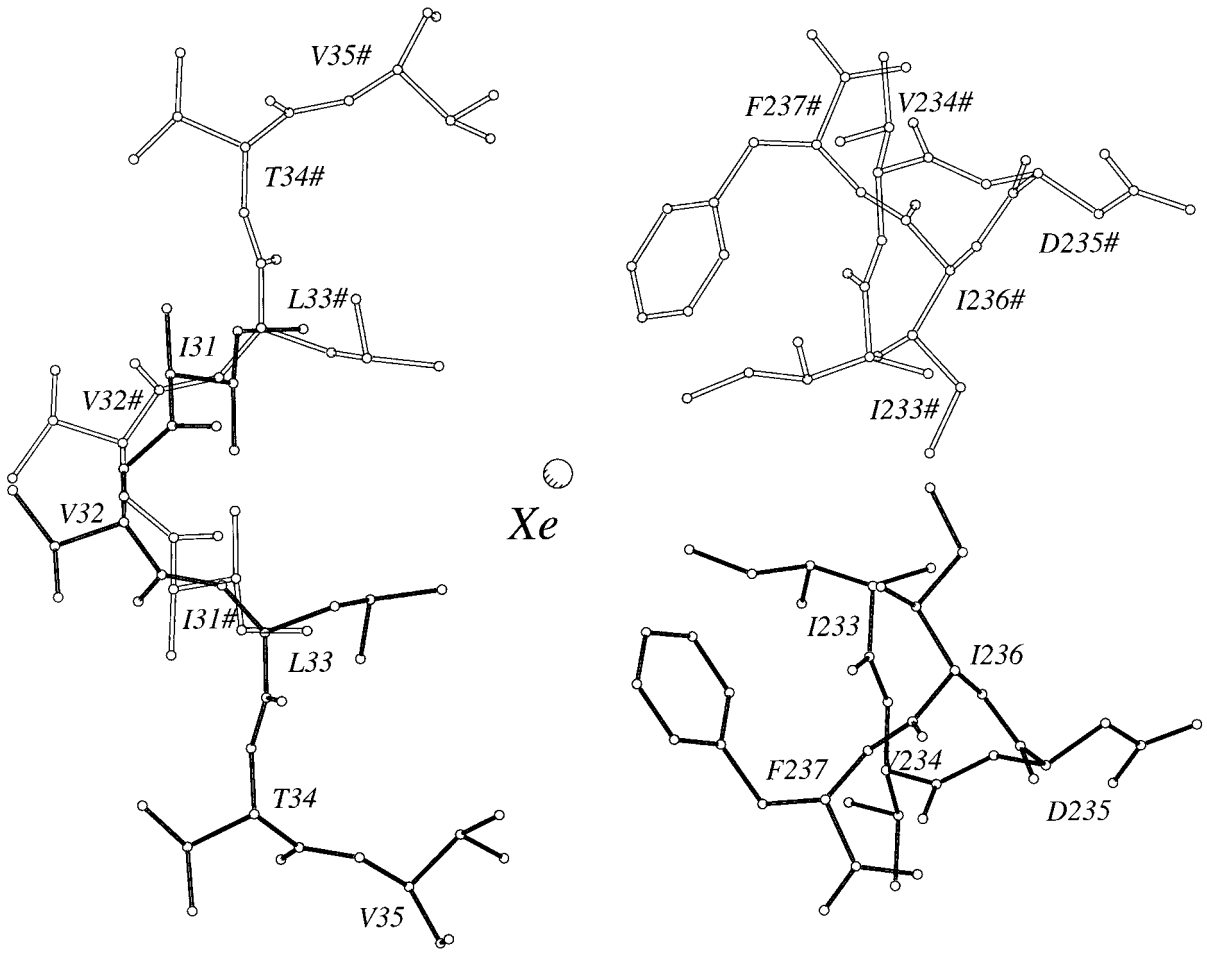


Fig. 3. δ-Endotoxin CytB: the intermolecular xenon binding site delimited by two symmetry-related molecules. The two-fold axis runs horizontally in the plane; the symmetry related molecule is in light tracing.

fix krypton. The smaller size of krypton atoms presumably also plays a role in this behaviour.

**Intra- vs. Inter-Hydrophobic Cavities: Lysozyme and CytB**

Xenon and krypton bind to hen egg lysozyme and CytB only to a moderate extent. In lysozyme, a difference-Fourier map reveals three sites and probably a fourth with a very low occupancy. Two of them (sites #1 and 4) are inter-molecular sites, located onto (or near to) a crystallographic two-fold axis, (direction [110]) and are located in cavities that are formed by the contact of symmetry-related molecules. The two other (sites #2 and 3) are intramolecular sites. The site #2 is a small spherical cavity deep in the inner core of the enzyme (Figs. 1, 2). In contrast, krypton binds solely to the intramolecular site, visible on Figure 1, with an occupancy of about 50%. In the case of the mosquitocidal δ-endotoxin CytB,[31] xenon binds into a closed intermolecular cavity at the dimer interface. In the crystal, this site lies on a crystallographic two-fold axis. (Fig. 3).

**Urate Oxidase Binding Site: A Probe for the Oxygen Binding?**

Urate oxidase from *Aspergillus flavus* is an enzyme that converts uric acid to allantoin with the aid of molecular oxygen. The unique binding site of xenon (Fig. 4) is nearly fully occupied.[8] The xenon atom is located near the active site of the enzyme. Hemoglobin was one of the first proteins shown to bind xenon. One might anticipate that many other enzymes, which are able to use molecular gas as one of their substrates like Ni/Fe hydrogenases, [71] nitrogenases, or hemoglobins, and known to contain hydrophobic channels or pockets, would be potentially good candidates for binding xenon, in (or near to) the regions involved in the enzymatic reaction or transport. As a consequence, xenon may be a useful probe in the elucidation of the mechanism of such enzymes.

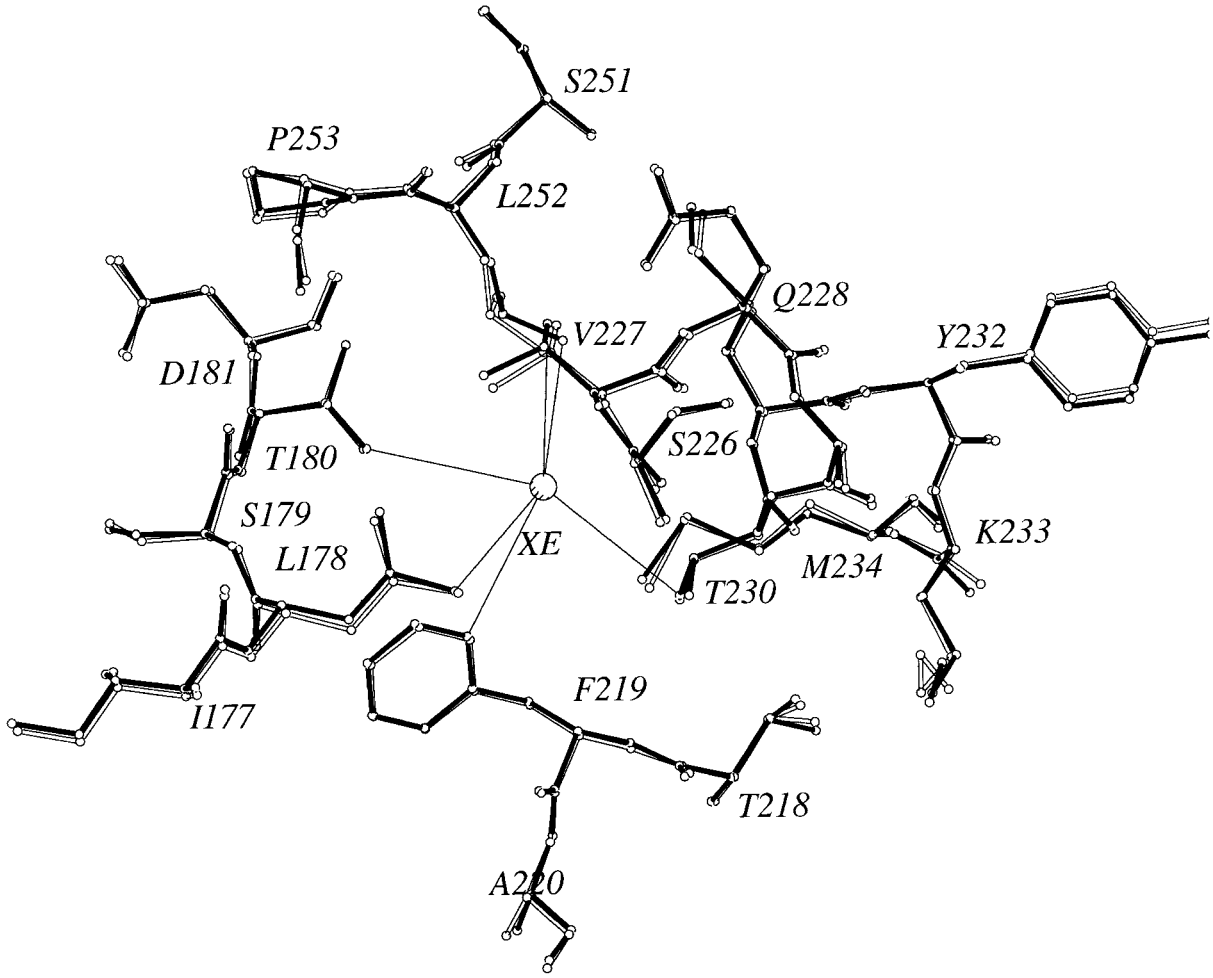


Fig. 4. Urate-oxidase: the xenon binding site. This cavity is in the vicinity of the active site of the enzyme which converts uric acid to allantoin using molecular oxygen. In light tracing, the refined native coordinates, in bold tracing, the refined xenon complex. This illustrates the negligible steric modification induced by the binding in this case (the average distances for atoms of the 20 residues in the vicinity of the xenon are c.a. 0.16 Å, only two times the r.m.s. deviations in the refined models: 0.08 Å).

### Inter-Helical Hydrophobic Pockets: The Case of P64k and RXR

α-Helices in cross-interactions usually lead to the building of super secondary motifs that minimize interactions.[7] Very often, hydrophobic side-chains, coming from different helices, are then brought into close contact to each other, delimiting pockets that may accommodate xenon atoms. Such pockets are observed in the P64k lipoamide dehydrogenase domain and in the RXR retinoic binding domain (Figs. 5, 6). In each crystal structure, two of these pockets are observed. In the case of P64k, a major (≅50%) and a minor site (30%) were found. In the case of RXR, the binding was so favorable that both sites were nearly fully occupied and the structure was solved mainly with the aid of this doubly labeled derivative. It is important to note that one of these cavities (site #1) corresponds to the putative ligand-binding site (pocket B in the description given by Bourguet et al.[3]).

### Xenon Binding to COMP: A Molecular Model for the Action of General Anesthetics?

COMP[34] is a unique example of multiple xenon binding sites in a channel-like structural motif. COMP forms a pentameric coiled coil with subunits constituted by α-helical structures. The hydrophobic axial pore of the pentameric bundle is filled with water molecules in the native state, but under a pressure of 10 bar, xenon atoms bind into the pore and displace some of the water molecules. A total of eight xenon atoms were refined at discrete binding sites, lining up the pore axis. We suggest that this xenon complex may provide a molecular model for the action of general anesthetics in postsynaptic ion channels. The molecular targets of general anesthet-

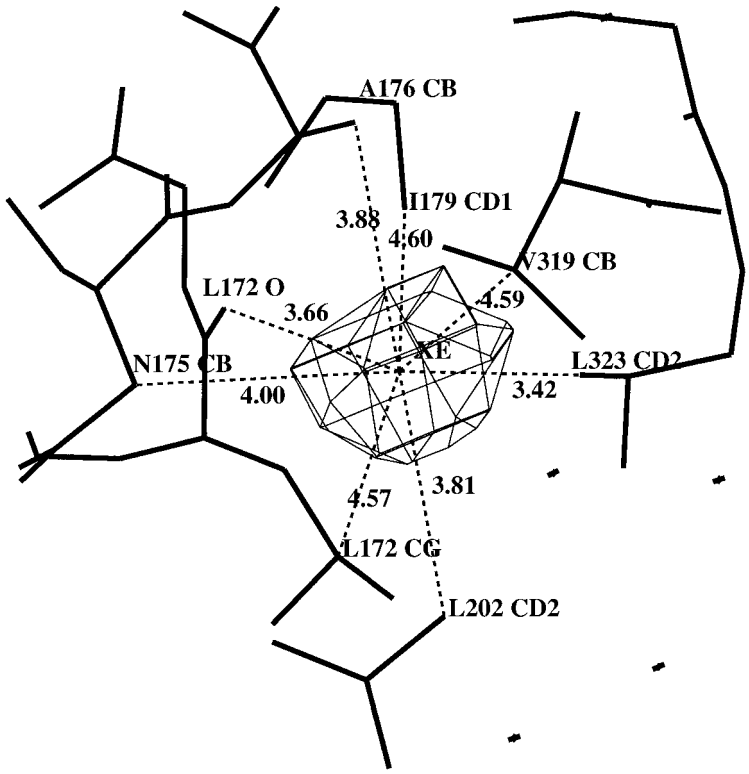


Fig. 5. P64k: the major binding site of xenon, with the refined model superimposed to the electron density (calculated with $||F_{deriv}| - |F_{native}||$ amplitudes and the refined phases; contouring is at 5 $\sigma$ above the mean density).

ics in the organism are still unknown[17,18,38] but there is evidence that anesthetic molecules inhibit the ion flux through the channel of ligand-gated postsynaptic receptors by binding to discrete protein sites.[80] Site-directed mutagenesis studies on the nicotinic Acetylcholine Receptor (nAchR) suggest that anesthetics bind directly to the channel pore.[81] The structure of COMP has marked similarities with proposed models of the nAchR and the observed discrete xenon binding sites in the channel pore of COMP[34] lend therefore strong support to the above-mentioned theory of the action of general anesthetics.

### The Special Case of the Serine Hydrolase Binding Sites

Serine hydrolases possess a unique catalytic motif built by the so-called catalytic triad (most commonly Ser-His-Asp). Apart from a few examples, all triads have similar spatial configurations while the rest of the protein folding may be completely different. The arrangement of the chain around the catalytic site delimits a binding crevice for the amino-acid to be cleaved, and is at the origin of the specificity of the enzyme. The character of this zone is usually hydrophobic, and indeed the xenon atom is observed bonded in this region. The four hydrolases we have investigated are able to fix xenon with a high occupancy in a single well-defined site. A superimposition of all catalytic triads complexed with the xenon positions is shown in Figure 7. For some of them, their binding sites have already been described[51]: the xenon (or krypton) atom is close to the O$\gamma$ of the active serine. It is located in the P1 site (following the nomenclature of Schechter and Berger[49]), with additional contacts towards a few hydrophobic residues, or towards polar atoms. In contrast to the small, closed hydrophobic cavities observed in the majority of proteins, the xenon binding sites in serine hydrolases are large solvent-accessible pockets that, in the cases of elastase, collagenase and cutinase contain ordered water molecules which are displaced upon xenon binding. Thus, apart from mapping hydrophobic cavities that are important in protein dynamics, xenon can also be used to detect potential substrate or ligand binding sites in proteins.

The role played by the catalytic serine is, in fact, not crucial for xenon binding. The S120A mutant of cutinase (where the active site serine is replaced by an alanine) still fixes the xenon at the same place and with equivalent occupancy.

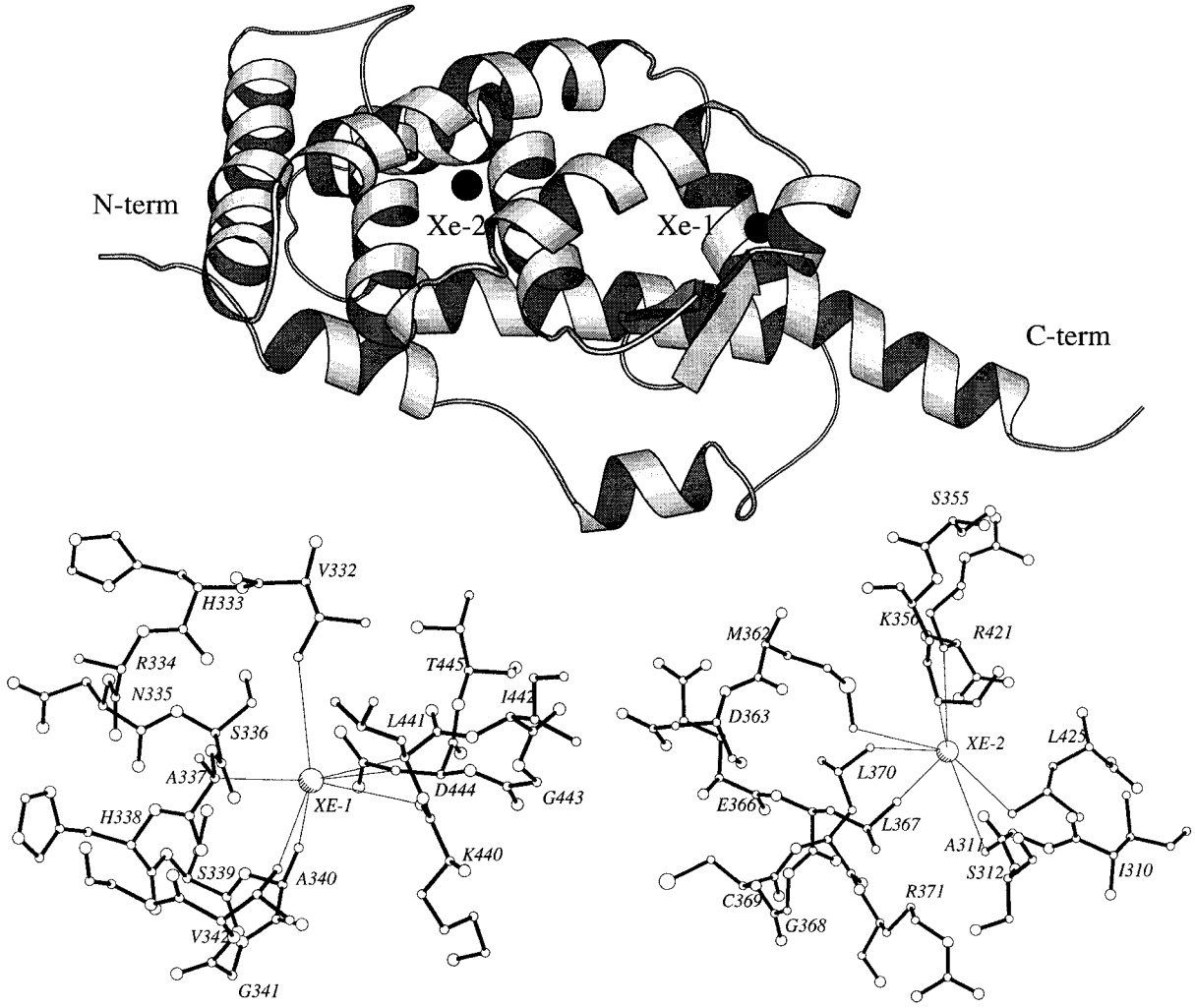


Fig. 6. RXR: locations of the xenon binding sites. The site #2 is delimited by residues coming from two helices. Site #1: the side chains which delimit the cavity belong to three different helices, the cavity is very small, and the xenon atom has a full occupancy. The schematic ribbon diagram of the molecule above indicates the location of the two sites.

**Xenon and Krypton as Heavy Atoms**

The recent interest in protein-xenon complexes has been prompted by the possibility of using them as heavy-atom derivatives for phase determination in macromolecular crystallography.[48,50,52,53,63,70] The crystal structures of RXR, DMSO-reductase, COMP, Photosystem I,[25] P64k, and urate-oxidase have been solved by the MIR method with isomorphous derivatives including xenon complexes. The structure of RXR was initially solved with a 5Å MIR map, based only on the xenon derivative. The α-helices of the structure were clearly visible in this initial map and a discontinuous polyalanine model could be traced. At a latter stage, data from a classical mercury derivative were added to improve the map. Because of its high degree of isomorphism, the xenon derivative has a significantly better phasing power than the mercury derivative.[3] Xenon derivatives are likely to bind to sites that are different from those of standard heavy atoms, which, like Hg or Pt, bind predominantly to specific functional groups. The structure of urate-oxidase illustrates this advantage[8]: only Hg and Pb derivatives of good quality had been obtained by standard soaking techniques, but the major binding sites of both cations were very close to each other, thus limiting the phasing power. The heavy-atom site in the xenon derivative is far away from the Hg and Pb sites, and thus improved the quality of the MIR phases.

The major advantage of xenon derivatives is their very high degree of isomorphism, but this notion should perhaps not be pushed too far. Local rearrangements of side-chains and displacements of water molecules may occur upon rare gas binding, as

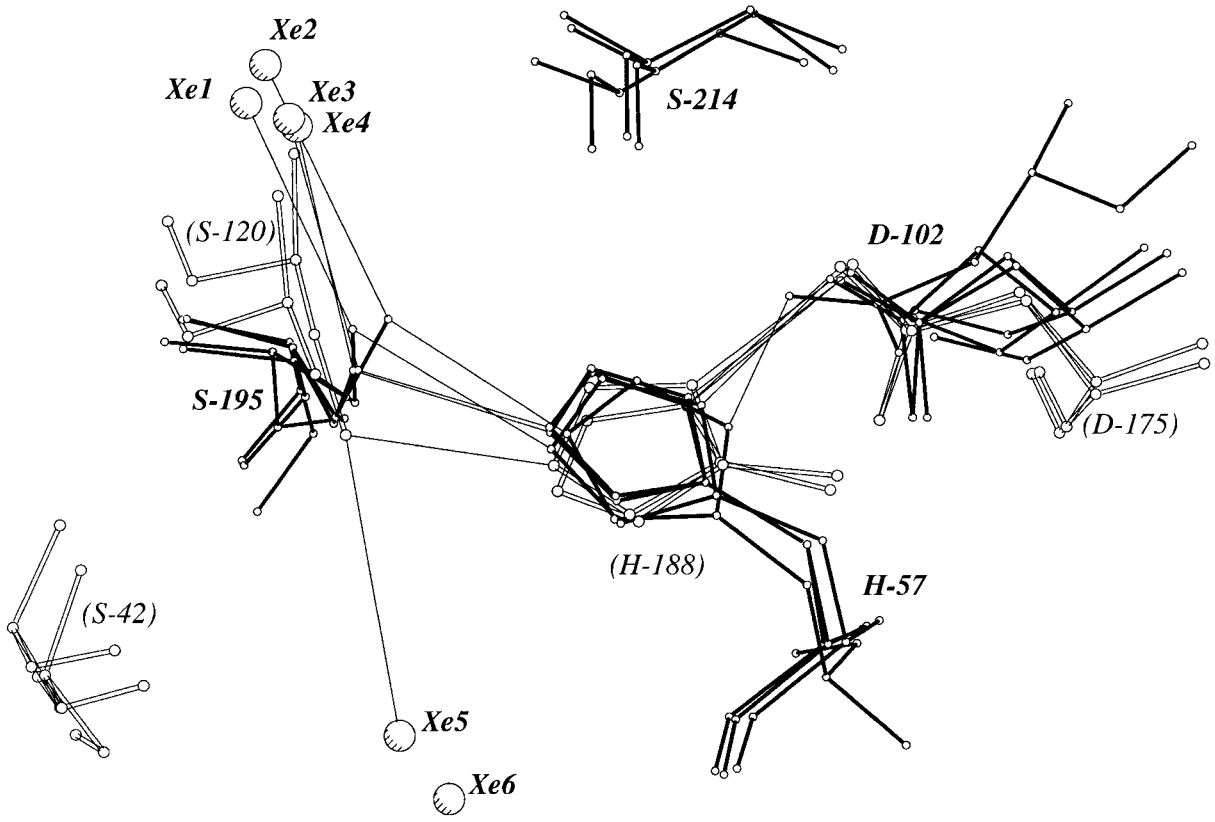


Fig. 7. Superimposition of the catalytic triads of elastase, subtilisin, cutinase (native and S120A mutant), and collagenase (two active sites). The least squares fit was performed using only the side chains of Ser195-His57-Asp102 (numbering refers to the standard chimotrypsin). The figure shows the refined position of the bonded xenon atoms in the five structures. Xenon positions are all within a sphere of 1Å, at a distance of ≅4Å away from the catalytic serine in proteinases (although not involved in the binding, the conserved Ser214 which lines the pocket border, is also represented). Note the special case of cutinase and its S120A mutant (light tracing); the hydrophobic pocket of this esterase is differently oriented with respect to the triad. The xenon still remains at close distance from Ser120 (or Ala120) but is no longer superimposable to the others. Xenon labeling: 1 = elastase; 2 = subtilisin; 3 and 4 = collagenase; 5 and 6 = cutinase, native and mutant.

was evidenced by a careful analysis of krypton binding to elastase.[52] Though these structural changes do only marginally impede the quality of the calculated SIRAS-phases, they show that the concept of gas binding into a pre-existing site, without any perturbation of the surrounding protein structure is only accurate in a first approximation. Binding of dichloromethane and cyclopropane to myoglobin is also shown to be accompanied by local structural rearrangements.[42,56,57] Stowell et al.[63] report on two cases where xenon derivatives were non-isomorphous, due to changes in cell parameters. They noticed that cell parameters did not change upon pressurization with nitrogen gas, and concluded that this effect is due to a strong binding or interaction between xenon and the protein. In the absence of a more detailed analysis, one can only speculate about the cause of this effect, but one plausible explanation would be that xenon binds to intermolecular cavities (as in lysozyme or CytB), thus inducing changes (or disruption) in the crystal lattice.

What size protein can be phased by xenon or krypton? The answer obviously depends on the number of heavy-atom sites but a single xenon site gave a useful derivative for DMSO-reductase, a 85kDa protein.[54] On the other hand, careful data collection and processing, as well as statistically optimal heavy-atom refinement and phasing, allowed the determination of a high-quality electron density map for elastase (26 kDa) from a single, half-occupied krypton atom.[52] From this, one can extrapolate that a single, fully occupied xenon atom can be used to produce a similar result with a 90 kDa protein. For larger structures, it is anticipated that more binding sites are required.

## CONCLUSION

In the present study, the binding of xenon and krypton to a large variety of proteins has been studied. Xenon is shown to bind to small hydrophobic pockets, accessible or buried in the core structure of the protein, usually without disturbing the folding of

the chains. Advantage can be taken to use this technique to detect such cavities in proteins.

In this study, we analyze in detail the binding sites of xenon and/or krypton in several proteins belonging either to the same class (serine proteinases) or from different origins. In almost all the cavities able to bind xenon, we observe predominant interactions with short hydrophobic side chains like leucine, isoleucine, valine, or alanine. This mapping of hydrophobic cavities is a powerful technique that complements NMR techniques in solution using stable isotopes of xenon ($^{129}$Xe and $^{131}$Xe). Finally, xenon has now become an attractive and useful heavy atom for preparing isomorphous derivatives in macromolecular crystallography.

## ACKNOWLEDGMENTS

This work was supported by grants from the CNRS/MR/CEA (Action Concertée des Sciences du Vivant 5) and a NATO grant for one of us (M.S.). We thank Drs. C. Cambillau (AFMB-CNRS, Marseille, France); A. Ducruix (LBS, Gif s/Yvette, France); D. Moras (IGMBC, Strasbourg, France); J.P. Mornon (LMCP, Paris, France); and Jade Li (LMB, MRC, Cambridge, UK), who participated at various stages of this study.

## REFERENCES

2. Bernstein, F.C., Koetzle, T.F., Williams, J.B., Meyer, E.F., Jr., Brice, M.D., Rodgers, J.R., Kennard, O., Shimanouchi, T., Tasumi, M. The protein data bank: A computer-based archival file for macromolecular structures. J. Mol. Biol. 112:535–542, 1977.
3. Bourguet, W., Ruff, M., Chambon, P., Gronemeyer, H., Moras, D. Crystal structure of the ligand binding domain of the human nuclear receptor RXRα. Nature 375:377–382, 1995.
4. Broutin, I., Arnoux, B., Riche, C., Lecroisey, A., Keil, B., Pascard, C., Ducruix, A. 1.8Å structure of *Hypoderma lineatum* collagenase: A member of the serine proteinase family. Acta Crystallogr. D 52:380–392, 1996.
5. Brünger, A.T., Krukowski, A., Erickson, J.W. Slow-coding protocols for crystallographic refinement by simulated Annealing. Acta Crystallogr. A46:585–593, 1990.
6. CCP4 Collaborative Computational Project, Number 4. Acta Crystallogr. D 50:760–764, 1994.
7. Chothia, C., Levitt, M., Richardson, D.C. Structure of proteins: Packing of α-helices and pleated sheets. Proc. Natl. Acad. Sci. U.S.A. 74:4130–4134, 1977.
8. Colloc'h, N., El Hajji, M., Bacchet, B., L'Hermite, G., Schiltz, M., Prangé, T., Castro, B., Mornon, J.-P. Crystal Structure of Urate Oxidase from Aspergillus flavus. Nature Struct. Biol. In press.
9. Conn, H.L. Equilibrium distribution of radio-xenon in tissue: Xenon-hemoglobin association curve. J. Appl. Physiol. 16:1065–1070, 1961.
10. Connolly, M.L. Analytical molecular surfaces calculation. J. Appl. Cryst. 16:548–558, 1983.
11. Cullen, S.C., Gross, E.G. The anesthetic properties of xenon in human and animal beings, with additional observations on krypton. Science 113:580–582, 1951.
12. Ewing, J.G., Maestas, S. The thermodynamics of absorption of xenon by myoglobin. J. Phys. Chem. 74:2341–2344, 1970.
13. Featherstone, R.M., Muehlbaecher, C.A. The current role of inert gases in the search for anesthesia mechanisms. Pharmacol. Rev. 15:97–121, 1963.
14. Featherstone, R.M., Settle, W. La pharmacologie des gaz rares. Actual. Pharmacol. 27:69–86, 1974.
15. Feher, V.A., Baldwin, E.P., Dahlquist, F.W. Access of ligands to cavities within the core of a protein is rapid. Nature Struct. Biol. 3:516–521, 1996.
16. Fourme, R., Dhez, P., Benoit, J.-P., Kahn, R., Dubuisson, J.-M., Besson, P., Frouin, J. Bent crystal, bent multilayer optics on a multipole wiggler line for an X-ray diffractometer with an imaging plate detector. Rev. Sci. Instrum. 63:982–987, 1992.
17. Franks, N.P., Lieb, W.R. What is the molecular nature of general anaesthetic target sites? Trends Pharmacol. Sci. 8:169–174, 1987.
18. Franks, N.P., Lieb, W.R. Molecular and cellular mechanisms of general anaesthesia. Nature 367:607–614, 1994.
19. Hendrickson, W.A., Konnert, J.H. Stereochemically restrained refinement of macromolecular structures. Methods Enzymol. 115:252–270, 1985.
20. Hermans, J., Shankar, S. The free energy of xenon binding to myoglobin from molecular dynamics simulation. Isr. J. Chem. 27:225–227, 1986.
21. Hubbard, S.J., Gross, K.H., Argos, P. Intramolecular cavities in globular proteins. Protein Eng. 7:613–626, 1994.
22. Klapper, M.H. On the nature of the protein interior. Biochim. Biophys. Acta 229:557–566, 1971.
23. Kocher, J.P., Prévost, M., Wodak, S.J., Lee, B. Properties of the protein matrix revealed by the free energy of cavity formation. Structure 4:1517–1529, 1996.
25. Krauß, N., Schubert, W.D., Klukas, O., Frome, P., Witt, H.T., Saenger, W. Photosystem I at 4Å resolution: A joint photosynthetic reaction center and core antenna system. Nature Struct. Biol. 3:965–973, 1996.
26. Kurinov, I.V., Harrison, R.W. The influence of temperature on lysozyme crystals. Structure and dynamics of protein and water. Acta Crystallogr. D 51:98–109, 1995.
27. La Fortelle, E., Bricogne, G. In: "Methods in Enzymology: Macromolecular Crystallography." Sweet, R.M., Carter, C.W. (eds.). New York: Academic Press, 1997:472–494.
29. Leslie, A.G.W. In: "Joint CCP4 and ESF-EACMB Newsletter on Protein Crystallography," Warrington: SERC Daresbury Laboratory, 26, 1992.
30. Lesser, I.M. Brain imaging in late-life psychosis. Curr. Opin. Psychiatry 7:354–357, 1994.
31. Li, J., Pandelakis, A., Koni, P.A., Ellar, D.J. Structure of the mosquitocidal δ-endotoxin CytB from *Bacillus thuringiensis* sp. *kyushuensis* and implications for membrane pore formation. J. Mol. Biol. 257:129–152, 1996.
32. Li de la Sierra, I., Prangé, T., Fourme, R., Padrón, G., Fuentes, P., Musacchio, A., Madrazo, J. Crystallisation and preliminary X-ray investigation of a recombinant outer membrane protein from *Neisseria meningitidis*. J. Mol. Biol. 235:1154–1155, 1994.
33. Li de la Sierra, I., Pernot, L., Prangé, T., Saludjian, P., Schiltz, M., Fourme, R., Padrón, G. Molecular structure of the Lipoamide dehydrogenase domain of a surface antigen from *Neisseria meningitidis*. J. Mol. Biol. 269:129–141, 1997.
34. Malashkevich, V.N., Kammerer, R.A., Efimov, V., Schulthess, T., Engel, J. The crystal structure of a five-stranded coiled-coil in COMP: A prototype ion channel? Science 274:761–765, 1996.
35. Martinez, C., De Geus, P., Lauwereys, M., Mathissens, G., Cambillau, C. *Fusarium solani* cutinase is a lypolytic enzyme with a catalytic serine accessible to solvent. Nature 356:615–618, 1992.
36. Martinez, C., De Geus, P., Lauwereys, M., Mathissens, G., Cambillau, C. Engineering cystein mutants to obtain crystallographic phases with a cutinase from *Fusarium solani pisi*. Protein Eng. 6:157–165, 1993.
37. Meyer, E.F., Cole, G.M., Radhakrishnan, R., Epp, O. Structure of native porcine pancreatic elastase at 1.65Å resolution. Acta Crystallogr. B 44:26–38, 1988.
38. Miller, K.W. The nature of the site of general anesthesia. Int. Rev. Neurobiol. 27:1–61, 1985.
39. Miller, K.W., Reo, N.V., Schoot Uiterkamp, A.J.M., Stengle, D.P., Stengle, T.R., Williamson, K.L. Xenon NMR: Chemical shifts of a general anaesthetic in common solvents,

proteins and membranes. Proc. Natl. Acad. Sci. U.S.A. 78:4946–4949, 1981.
40. Morton, A., Matthews, B.W. Specificity of ligand binding in a buried nonpolar cavity of T4 lysozyme: Linkage of dynamics and structural plasticity. Biochemistry 34:8576–8588, 1995.
42. Nunes, A.C., Schoenborn, B.P. Dichloromethane and myoglobin function. Mol. Pharmacol. 9:835–839, 1973.
43. Otwinowski, Z. Maximum likelihood refinement of heavy atom parameters. In: "Isomorphous Replacement and Anomalous Scattering." Proceedings of the CCP4 Study Weekend, January 25–26, 1991. Wolf, W., Evans, P.R., & Leslie, A.G.W. (eds.). Warrington: SERC Daresbury Laboratory, 1991:80–86.
44. Petsko, G.A., Tsernoglou, D. The structure of subtilopeptidase, 1. X-ray crystallographic data. J. Mol. Biol. 106:453–456, 1976.
45. Quilin, M.L., Baase, W.A., Matthews, B. Binding of small electron-dense ligands in large protein cavities. XVII Congress and General Assembly of the International Union of Crystallogr., Seattle, WA. Abstract PS04.14.17 in: Acta Crystallogr. A52: C-215, 1996.
47. Sachsenheimer, W., Pai, E.F., Schultz, G.E., Schirmer, R.H. Halothane binds in the adenine-specific niche of crystalline adenylate kinase. FEBS Lett. 79:310–312, 1977.
48. Sauer, O., Schmidt, A., Kratky, C. Freeze-trapping isomorphous xenon derivatives of protein crystals. J. Appl. Cryst., (in press).
49. Schechter, I., Berger, A. On the size of the active site in proteases. Biochem. Biophys. Res. Commun. 27:157–162, 1967.
50. Schiltz, M., Prangé, T., Fourme, R. On the preparation and X-ray data collection of isomorphous xenon derivatives. J. Appl. Cryst. 27:950–960, 1994.
51. Schiltz, M., Fourme, R., Broutin, I., Prangé, T. The catalytic site of serine proteinases as a specific binding cavity for xenon. Structure 3:309–316, 1995.
52. Schiltz, M., Shepard, W., Fourme, R., Prangé, T., de la Fortelle, E., Bricogne, G. High-pressure krypton gas and statistical heavy-atom refinement: A successful combination of tools for macromolecular structure determination. Acta Crystallogr. D 53:78–92, 1997.
53. Schiltz, M., Kvick, Å, Svensson, O.S., Shepard, W., de la Fortelle, E., Prangé, T., Kahn, R., Bricogne, G., Fourme, R. Protein crystallography at ultra-short wavelengths: Feasibility study of anomalous dispersion experiments at the xenon K-edge. J. Synchr. Rad. (in press).
54. Schindelin, H., Kisker, C., Hilton, J., Rajagopalan, K.V., Rees, D.C. Crystal structure of DMSO reductase: Redox-linked changes in molybdopterin coordination. Science 272:1615–1621, 1996.
55. Schoenborn, B.P. Binding of xenon to horse haemoglobin. Nature 208:760–762, 1965.
56. Schoenborn, B.P. Binding of cyclopropane to sperm whale myoglobin. Nature 214:1120–1122, 1967.
57. Schoenborn, B.P. Binding of anesthetics to proteins: An X-ray crystallographic investigation. Fed. Proc. Fed. Am. Soc. Exp. Biol. 27:888–894, 1968.
58. Schoenborn, B.P. Structure of alkaline metmyoglobin-xenon complex. J. Mol. Biol. 45:297–303, 1969.
59. Schoenborn, B.P., Featherstone, R.M. Molecular forces in anesthesia. Adv. Pharmacol. 5:1–17, 1967.
60. Schoenborn, B.P., Nobbs, C.L. The binding of xenon to sperm whale deoxymyoglobin. Mol. Pharmacol. 2:495–498, 1966.
61. Settle, W. Function of the myoglobin molecule as influenced by anesthetic molecules. In: "Guide to Molecular Pharmacology-Toxicology." Featherstone, R.M. (ed.). New York: Marcel Dekker, 1973.
62. Steinrauf, L.K. Preliminary X-ray data for some new crystalline forms of β-lactoglobulin and hen egg-white lysozyme. Acta Crystallogr. 12:77–79, 1959.
63. Stowell, M.H.B., Soltis, S.M., Kisker, C., Peters, J.W., Schindelin, H., Rees, D.C., Cascio, D., Beamer, L., Hart, P.J., Wiener, M.C., Whitby, F.G. A simple device for studying macromolecular crystals under moderate gas pressures (0.1–10 MPa). J. Appl. Cryst. 29:608–613, 1996.
64. Tilton, R.F., Kuntz, I.D. Nuclear magnetic resonance studies of xenon-129 with myoglogin and haemoglobin. Biochemistry 21:6850–6857, 1982.
65. Tilton, R.F., Petsko, G.A. A structure of sperm whale myoglobin at a nitrogen gas pressure of 145 atmospheres. Biochemistry 27:6574–6582, 1988.
66. Tilton, R.F., Kuntz, I.D., Petsko, G.A. Cavities in proteins: Structure of a metmyoglobin-xenon complex solved to 1.9Å. Biochemistry 23:2849–2857, 1984.
67. Tilton, R.F., Singh, U.C., Weiner, S.J., Connolly, M.L., Kuntz, I.D., Kollmann, P.A., Max, N., Case, D.A. Computational studies of the interaction of myoglobin and xenon. J. Mol. Biol. 192:443–456, 1986.
68. Tilton, R.F., Singh, U.C., Kuntz, I.D., Kollman, P.A. Protein-ligand dynamics. A 96 picosecond simulation of a myoglobin-xenon complex. J. Mol. Biol. 199:195–211, 1988.
70. Vitali, J., Robbins, A.H., Almo, S.C., Tilton, R.F. Using xenon as a heavy atom for determining phases in sperm whale met-myoglobin. J. Appl. Cryst. 24:931–935, 1991.
71. Montet, Y., Amara, P., Volbeda, A., Vernede, X., Hatchikian, E.C., Field, M.J., Frey, M., Fontecilla-Camps, J.C. Gas access to the active site of Ni-Fe hydrogenases probed by X-ray crystallography and molecular dynamics. Nature Struct. Biol. 4:523–526, 1997.
72. Wolfenden, R., Radzicka, A. On the probability of finding a water molecule in a non-polar cavity. Science 265:936–937, 1994.
74. Zhang, L.I., Hermans, J. Hydrophilicity of cavities in proteins. Proteins 24:433–438, 1996.
75. Schoenborn, B.P., Watson, H.C., Kendrew, J.C. Binding of xenon to sperm whale myoglobin. Nature 207:28–30, 1965.
76. Seeman, P. The Membrane Actions of Anesthetics and Tranquilizers. Pharmacol. Rev. 24:583–655, 1972.
77. Albert, M.S., Cates, G.D., Driehuys, B., Happer, W., Saam, B., Springer, C.S. Jr, Wishnia, A. Biological magnetic resonance imaging using laser-polarized. $^{129}$Xe. Nature 370:199–201, 1994.
78. Fitzpatrick, P.A., Steinmetz, A.C.U., Ringe, D., Klibanov, A.M. Enzyme Crystal Structure in a Neat Organic Solvent. Proc. Natl. Acad. Sci. USA 90:8653–8657, 1993.
79. Schoenborn, B.P., Featherstone, R.M., Vogelhut, P.O. Süsskind, C. Influence of Xenon on Protein Hydration as measured by a Microwave Absorption Technique. Nature 202:695–696, 1964.
80. Woods, S.C., Tonner, P.H., De Armendi, A.J., Bugge, B., Miller, K.W. Channel Inhibition by Alkanols occurs at a Binding Site on the Nicotinic Acetylcholine Receptor. Mol. Pharmacol. 47:121–130, 1995.
81. Forman, S.A., Miller, K.W., Yellen, G.A. Discrete Site for General Anesthetics on a Postsynaptic Receptor. Mol. Pharmacol. 48:574–581, 1995.